Characterization of Decommissioned PWR Vessel Internals Material Samples

Tensile and SSRT Testing (Nonproprietary Version)

This report describes research sponsored by EPRI and the U.S. Department of Energy (Award No. DE-FC07-00NE22796).

Technical Report

Characterization of Decommissioned PWR Vessel Internals Material Samples

Tensile and SSRT Testing (Nonproprietary Version)

1011027

Topical Report, September 2004

Cosponsor
U.S. Department of Energy,
Nuclear Energy Plant Optimization (NEPO)
Office of Nuclear Energy, Science and Technology
1000 Independence Avenue, S.W.
Washington, D.C. 20585-1290

EPRI Project Manager
H.T. Tang

EPRI • 3412 Hillview Avenue, Palo Alto, California 94304 • PO Box 10412, Palo Alto, California 94303 • USA
800.313.3774 • 650.855.2121 • askepri@epri.com • www.epri.com

DISCLAIMER OF WARRANTIES AND LIMITATION OF LIABILITIES

ORGANIZATION(S) THAT PREPARED THIS DOCUMENT

Westinghouse Electric Company, LLC

EPRI

ORDERING INFORMATION

Requests for copies of this report should be directed to EPRI Orders and Conferences, 1355 Willow Way, Suite 278, Concord, CA 94520, (800) 313-3774, press 2 or internally x5379, (925) 609-9169, (925) 609-1310 (fax).

CITATIONS

This report was prepared by

Westinghouse Electric Company, LLC
Science and Technology Department
1310 Beulah Road
Pittsburgh, PA 15235

Principal Investigators
M. Krug
R. Shogan

This report describes research sponsored by EPRI and the U.S. Department of Energy (Award No. DE-FC07-00NE22796. Task FY02 3-27).

The report is a corporate document that should be cited in the literature in the following manner:

Characterization of Decommissioned PWR Vessel Internals Material Samples: Tensile and SSRT Testing (Nonproprietary Version), EPRI, Palo Alto, CA: 2004. 1011027.

PRODUCT DESCRIPTION

Pressurized water reactor (PWR) cores operate under extreme environmental conditions due to coolant chemistry, operating temperature, and neutron exposure. Extending the life of PWRs requires detailed knowledge of the changes in mechanical and corrosion properties of the structural austenitic stainless steel components adjacent to the fuel (internals) subjected to such conditions. This project studied the effects of reactor service on the mechanical and corrosion properties of samples of baffle plate, former plate, and core barrel from a decommissioned PWR.

Results & Findings

Tensile testing revealed that both the yield strength and ultimate tensile strength of annealed 304SS at room temperature increase as a result of neutron irradiation. Irradiation causes an increase of approximately 400% in the yield strength and 80% in the ultimate tensile strength at approximately 5 dpa, at which point the strength increase is nearly saturated. At 608°F (320°C) irradiation causes an increase of approximately 500% in the yield strength and 190% in the ultimate tensile strength at approximately 5 dpa, at which point the strength increase is nearly saturated. At room temperature, and for high levels of neutron irradiation, the yield strength and ultimate tensile strength become similar; but yielding and necking do not coincide. Specimens having the highest levels of irradiation failed intergranularly. At the elevated temperature (608°F, 320°C), the yield point coincided with the onset of necking. Material strength at elevated temperature was lower than at room temperature. At elevated temperature there is a marked decrease in ductility compared with room temperature, but all specimens failed in a ductile manner.

SSRT (Slow Strain Rate Test) testing in simulated PWR water showed that both intergranular and transgranular cracking occurred in the low fluence specimens though intergranular cracks generally transitioned to transgranular before final ductile overload. A significant portion of the fracture surface of the nearly unirradiated specimen indicated a brittle failure mechanism. Percentages of both intergranular and transgranular fracture surface decreased between the nearly unirradiated specimens and those having ~0.5 dpa though this finding may be within the range of data scatter inherent in the SSRT. For neutron fluences above ~0.5 dpa, no transgranular cracking was observed; and intergranular cracking increased to values between approximately 20 and 30 percent. Nearly all observable surface cracks initiated on grooves from lathe machining.

Challenges & Objectives

Tensile testing provided information about the macroscopic effects of irradiation-induced microstructural changes in the program materials. SSRT testing involved strict control of environmental variables including chemistry and temperature and the maintenance of a constant extension rate throughout the duration of the test. The test results provide a measure of the evolution of IASCC (Irradiation Assisted Stress Corrosion Cracking) susceptibility with neutron fluence.

Applications, Values & Use

The tensile results presented in this report offer a starting point for understanding what is believed to be a strain-induced phase transformation in the program materials that affects their mechanical and chemical (corrosion) properties. Subsequent tests on the program material—fracture toughness, crack initiation, crack growth rate—rely on accurate measures of the tensile properties in order to select appropriate testing parameters.

SSRT testing provides valuable data describing the susceptibility of irradiated 304SS to stress corrosion cracking. These data will be added to the industry database to be used in making predictions about material durability in the reactor core environment. Future detailed analyses of these data are planned to determine if other useful metrics besides percent brittle failure of the fracture surface exist for measuring IASCC susceptibility. Such metrics, if identified, may help elucidate the underlying mechanisms responsible for IASCC failures.

EPRI Perspective

The tests conducted in this project provide quantitative information on the mechanical properties of irradiated 304SS. Two versions of reports are published to document the results; this non-proprietary version provides a summary and a related proprietary version, EPRI report 1008205, contains detailed results and data. This program represents the first time that significant amounts of PWR internals have been available to allow the effects of reactor service on the materials' mechanical and corrosion properties to be determined. Related EPRI reports include Materials Reliability Program: Determination of Operating Parameters of Extracted Bolts - MRP-52 (1003076), Materials Reliability Program: Hot Cell Testing of Baffle /Former Bolts Removed From Two Lead Plants - MRP-51 (1003069), and Materials Reliability Program: Characterizations of Type 316 Cold Worked Stainless Steel Highly Irradiated Under PWR Operating Conditions - MRP 73 (1003525).

Approach

Tensile testing was completed in a hot cell in air. Tests were run both at room temperature and at 608°F (320°C) using a three-zone electric resistance split-tube furnace with a 9-inch (23 cm) hot zone. Data were recorded digitally and autographically. SSRT testing was conducted at a constant strain rate of $1x10^{-7}$ mm/mm in a shielded autoclave at 644°F (340°C) in simulated reactor coolant chemistry. Data were recorded digitally for determination of the stress-strain behavior. Fractography of the failed specimens was performed using a shielded Amray Scanning Electron Microscope.

Keywords

Pressurized water reactor
Radiation effects
Tensile
Slow Strain Rate Tensile (SSRT)
Reactor Internals
Stainless Steel
Irradiation Assisted Stress Corrosion Cracking (IASCC)

ABSTRACT

Pressurized water reactor (PWR) cores operate under extreme environmental conditions due to coolant chemistry, operating temperature, and neutron exposure. Extending the life of PWRs requires detailed knowledge of the changes in mechanical and corrosion properties of the structural austenitic stainless steel components adjacent to the fuel (internals) that are inherent to such conditions. This program represents the first time that significant amounts of PWR internals have been available to allow the effects of reactor service on the materials' mechanical and corrosion properties to be determined. This report contains the results of room temperature and elevated temperature tensile testing and of elevated temperature slow strain rate tensile corrosion testing (SSRT) of samples machined from decommissioned reactor internals.

Tensile testing revealed that the yield strength and ultimate tensile strength of annealed 304SS at room temperature both increase as a result of neutron irradiation. Unirradiated values for room temperature yield strength and ultimate tensile strength (from the retrieved material certification sheets) are $\sigma_Y \approx$ 35 ksi (240 MPa), T.S. $\approx$ 80 ksi (550 MPa), respectively. Irradiation causes an increase of approximately 400% in the yield strength and 80% in the ultimate tensile strength at approximately 5 dpa, at which point the strength increase is nearly saturated. Unirradiated values for yield strength and ultimate tensile strength at 608°F (320°C) (by testing nearly unirradiated program material) are $\sigma_Y \approx$ 25 ksi (170 MPa), T.S. $\approx$ 65 ksi (450 MPa). Irradiation causes an increase of approximately 500% in the yield strength and 190% in the ultimate tensile strength at approximately 5 dpa, at which point the strength increase is nearly saturated. At room temperature, and for high levels of neutron irradiation, the yield strength and ultimate tensile strength become similar, but yielding and necking do not coincide as a result of the high ductility enabled by a martensitic phase transformation from the austenitic parent phase. Specimens having the highest levels of irradiation failed intergranularly. At elevated temperature (608°F, 320°C) there appeared to be very little or no martensitic phase transformation, and the yield point coincided with the onset of necking. Material strength at elevated temperature was lower than at room temperature. At elevated temperature there is a marked decrease in ductility compared with room temperature, however all specimens failed in a ductile manner. There is little change in properties as measured by tensile specimens of different sizes, in strength or in ductility. Tensile properties measured with the miniature gage diameter specimens may be regarded as typical of those that would be obtained with a larger specimen design.

SSRT testing in simulated PWR water showed that both intergranular and transgranular cracking occurred in the low fluence specimens. A significant portion of the fracture surface of the nearly unirradiated indicated a brittle failure mechanism. Percentages of both intergranular and transgranular fracture surface decreased between the nearly unirradiated specimens and those having ~0.5 dpa, however this may be within the range of data scatter inherent in the SSRT test. For neutron fluences above ~0.5 dpa, no transgranular cracking was observed, and intergranular cracking increased to values between approximately 20 and 30 percent. Cracking in low-fluence specimens began as either transgranular or intergranular. Intergranular cracks generally transitioned to transgranular before final ductile overload.

CONTENTS

LIST OF FIGURES

LIST OF TABLES

1
OBJECTIVE

The program to test and characterize reactor internals material samples harvested from a decommissioned PWR consists of several parts. The objectives of the part of the program that is documented in this report can be summarized as follows:

- Develop a database of tensile and SSRT data for Type 304 stainless steel plate irradiated in the internals region of a PWR.
- Compare the program Type 304 data with similar data for other austenitic stainless steels and from other irradiation sources to allow a determination of which data sets can be applied to PWR use.
- Study irradiation effects on PWR vessel internals components for extended plant operation beyond its designed life.
- Provide data for PWR owners and regulators to justify plant life extension.

2
INTRODUCTION

Austenitic stainless steels were selected for the internals structures surrounding the core in the PWR design because of their relative strength, ductility and resistance to corrosion in the PWR water environment. Recently, studies have shown that the neutron radiation environment affects this corrosion resistance.[1,2] A few actual failures of internals bolting as well as of similar alloys used for control rod sheathing have been reported.[3,4] These failures have led to studies of irradiation effects on stainless steels, particularly for bolting applications. The alloys studied were mostly Types 316 and 347 since they were available after bolt or bottom mounted instrument tube replacement. Few studies included Type 304 at high fluence levels since it is used for larger structures not easily removed. Irradiation effects in Type 304 are of particular interest, however, since most of the reactor internals are constructed of this alloy and BWR experience shows that it is susceptible to irradiation assisted stress corrosion cracking (IASCC).

In addition Type 304 stainless steel is the austenitic alloy most susceptible to irradiation induced void swelling from breeder reactor experience. While little evidence of significant swelling has been found in other PWR austenitic stainless steel alloys irradiated to high fluence, Type 304 material has generally not been available for study.

When sections of stainless steel from the internals region became available during the decommissioning of a PWR reactor, the EPRI MRP Internals Task Group was able to obtain material for detailed characterization. Studies planned for these materials include:

- Thermal and irradiation history calculations
- Tensile properties
- Fracture toughness measurements
- SSRT testing to measure IASCC (Irradiation Assisted Stress Corrosion Cracking) susceptibility
- Corrosion crack initiation

---

[1] Conermann, J., Shogan, R., International IASCC Advisory Committee, Phase 2 Final Report, Westinghouse Electric Co. LLC, January, 2004.

[2] *Material Reliability Program: Hot Cell Testing of Baffle/Former Bolts Removed From Two Lead PWR Plants (MRP-51)*, EPRI, Palo Alto, CA: 2001.1003069.

[3] Matsuoka, T., et al., Performance of PWR RCCA Rodlets Regarding Cladding Tube Cracking Caused by Absorber Swelling, Proceedings of ICON 5, 5th International Conference on Nuclear Engineering, May 26-30, 1997, Nice, France.

[4] Sipush, P. J., et al., Lifetime of PWR Silver-Indium-Cadmium Control Rods, EPRI-NP-4512.

- Corrosion crack growth
- Microstructural studies to correlate microstructural changes with mechanical and corrosion property changes
- Swelling measurements

The program materials were taken from the baffle, former, barrel and baffle-former bolts of the decommissioned reactor. All of these components were constructed of Type 304 stainless steel. Background information about the materials and sections obtained for study and their calculated thermal and fluence histories was previously reported [1]. In this report the tensile testing and SSRT testing of the decommissioned materials will be described and the results reported.

2.1 References

1. Characterization Report.

3
TENSILE TESTING

Tensile testing provides an assessment of the amount of radiation induced matrix damage incurred by the program materials. Typically the tensile yield and ultimate strengths increase with increasing irradiation level. This effect saturates after several dpa neutron exposure (1 dpa (displacement per atom during the irradiation time) corresponds to ~$7x10^{20}$ n/cm^2, E>1MeV). Reduction of area does not normally significantly decrease with irradiation; however non-uniform elongation takes place in a diminishing fraction of the reduced section which results in rapid necking and an overall decrease in total elongation.

3.1 Specimen Design

In this study tensile tests were manufactured from the baffle, former and barrel plates at a range of neutron exposure levels. The objective was to obtain properties as a function of fluence and to determine the heat-to-heat variability of the irradiation effect. All but one of the test specimens were subsized relative to ASTM recommended sizes (Figure 3-1) because of the volume of available material and the property gradients expected because of neutron fluence gradients. The gage length to diameter ratio was kept at 4-to-1 as recommended by ASTM E8 [2]. Additionally, a more standard 0.25 inch (6.35 mm) gage diameter specimen (Figure 3-2) was machined from the former plate for comparison with a 0.110 inch (2.79 mm) diameter specimen of similar radiation environment and material as a means of validating the use of the miniature size specimens to evaluate materials properties.

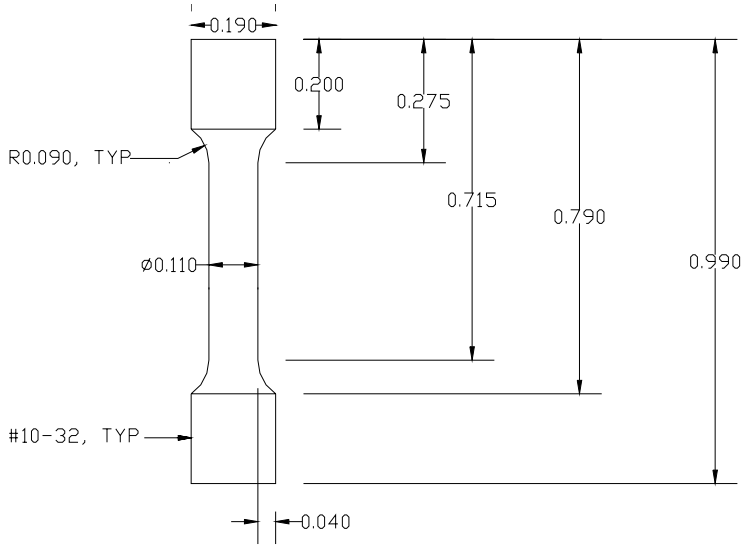

Figure 3-1
Diagram of Small Diameter Tensile Test Specimen with 2.78 mm Gage Diameter (Units in Inches)

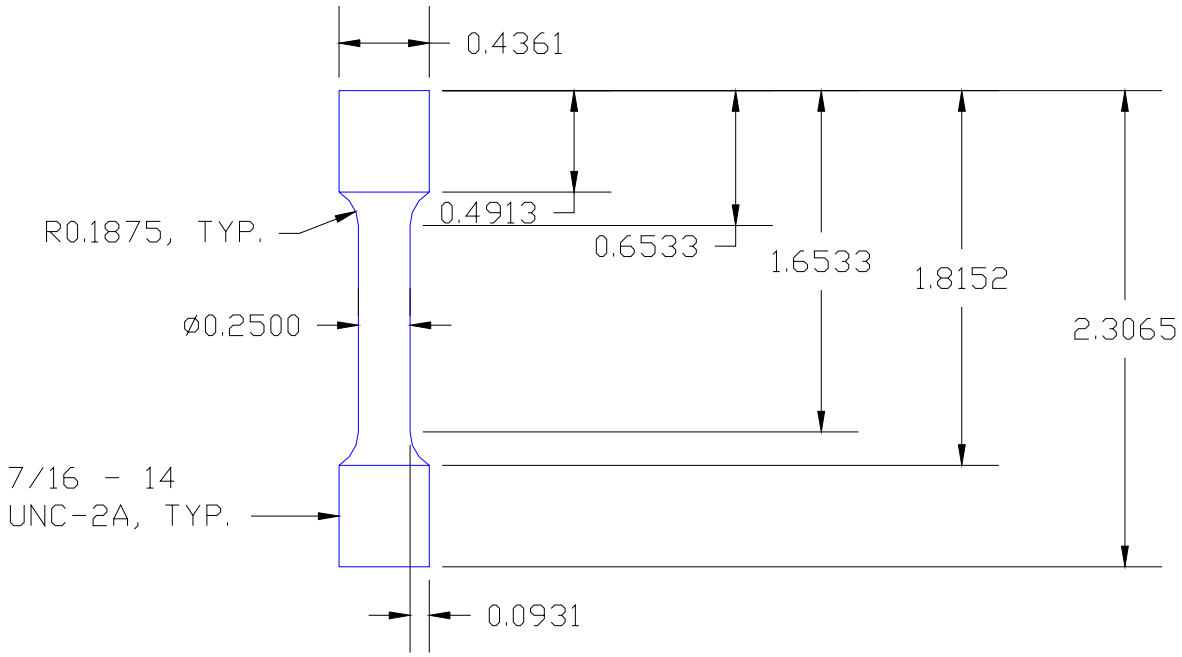

Figure 3-2
Diagram of the Large Diameter Tensile Specimen with 6.35 mm Gage Diameter (Units in Inches)

3.2 Specimen Machining

All post-irradiation machining was completed at the Westinghouse Science and Technology Department (STD) hot cell facility. Each specimen was given identification based on its origin: baffles were arbitrarily numbered 1-4, the former section is 5, and the barrel section is 6. Remaining characters in the specimen ID refer to the section of baffle, former, of barrel from which the specimen was removed.

Thirteen tensile specimens were machined in total. The machining process involved several steps. First, rough blanks were cut from the bulk material with a band saw. In instances where a minimal amount of material was available, a very thin diamond saw was used to make finer cuts. Specimen blanks were cut from the plates, maintaining original location and orientation within the internals section. These blanks were then machined in a remote, hot cell CNC lathe to their final configuration. Threaded ends and a reduced diameter section in the middle were turned into each of the rods, and a finishing die was run over the threaded ends. The reduced section was cut into the specimen taking 0.005 inch (0.1 mm) cuts at each pass and then making a final 0.002 inch (0.05 mm) pass. The rotating speed was approximately 500 rpm and feed rate was 0.005 inch/revolution (0.1 mm/rev).

Final specimen gage diameters were measures and found to be within +0.0006 (+0.02 mm) and -0.0025 inches (0.064 mm) of the drawing specifications. Actual measurements were used in the property calculations. Typical finished, machined specimens are shown in Figure 3-3.

The location of the specimens in the plate materials is shown in Appendix A.

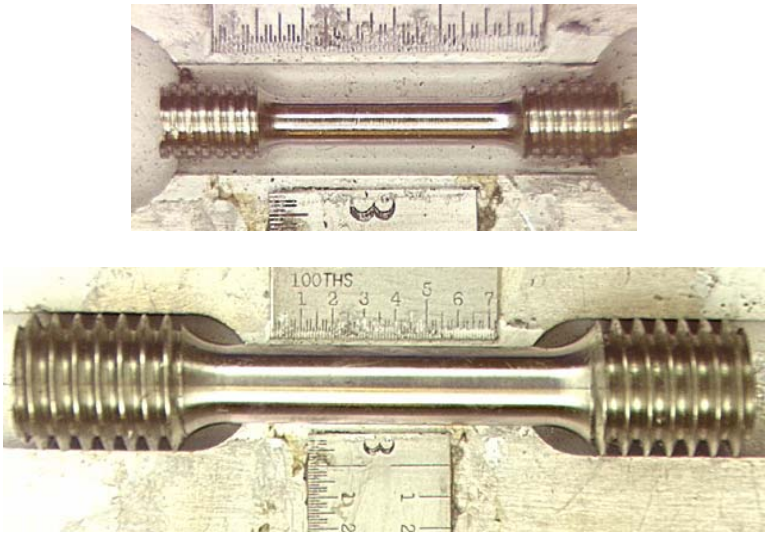

Figure 3-3
Photographs of the Two Typical Tensile Test Specimen Types at Approximately Actual Size

3.3 Tensile Testing Procedure

The tensile tests were performed on a 20,000 pound Instron split console test machine (Model 1115) with a digital upgrade, per applicable portions of ASTM Specifications E8 [2] and E21 [3]. Tests were run under constant crosshead displacement at a rate of 0.02 inch/minute (0.5 mm/min) for the 0.110 inch specimens, and 0.045 inch/minute (1.1 mm/min) for the 0.250 inch specimen. Data were recorded both digitally and autographically. Three test temperatures were used: room temperature 70°F, (21°C) 320°F (160°C) and 608°F (320°C). The elevated temperature tests were performed in a three-zone electric resistance split-tube furnace with a 9-inch hot zone. All tests were conducted in air.

As the small specimen size precluded use of a clip gage, elongation was measured via cross-head displacement and the use of an "effective" specimen gage length. The yield strength and ultimate tensile strength were measured directly from the load-extension curve using the original cross-sectional area, measured with a micrometer to the nearest 0.0001 inch (0.003 mm). Uniform elongation was measured from the load-extension curve as the percent increase in the length of the gage section at the onset of necking (maximum load) due to plastic deformation. Acknowledgement of the coincidence of necking and maximum load is standard industry practice. Total elongation was measured similarly at failure. Reduction in area was calculated as the percent change in cross-sectional area at failure; final cross-sectional area was determined from photographs of the specimen using a calibrated measurement feature in the laboratory's imaging software.

3.4 Tensile Testing Results and Discussion

Macro-photographs of the tested tensile specimens are shown in Figure 3-4.

Specimen 3F1 tested at 70°F

Specimen 3C1 tested at 70°F

Specimen 1H1 tested at 70°F

Specimen 1E1 tested at 70°F

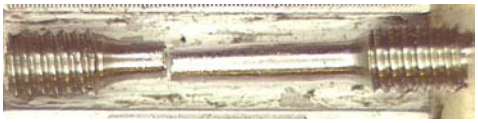

Specimen 5A2A1 tested at 70°F

Specimen 3C2 tested at 320°F

Specimen 3F2 tested at 608°F

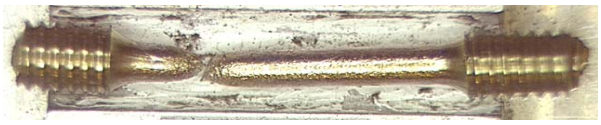

Specimen 3E1 tested at 608°F

Specimen 6C1 tested at 608°F

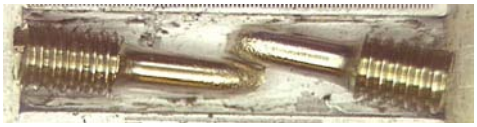

Specimen 1H2 tested at 608°F

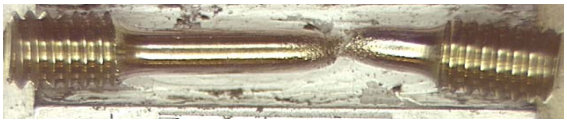

Specimen 1E2 tested at 608°F

Specimen 5A2A2 tested at 608°F

Specimen 5A2 tested at 608°F

Figure 3-4
Post-test Specimen Photographs

3.4.1 Strength

Neutron irradiation produced significant increases in strength in the program materials. Typically, well annealed Type 304 stainless steel yields at about 35 to 40 ksi (240 to 275 MPa) at room temperature. The very low fluence (<0.1 dpa) specimen tests confirmed this strength level. The yield strength increased with increasing neutron fluence showing a trend towards saturation above about 5 dpa. At the saturation fluence the yield strength had increased by about 400% at room temperature and 500% at 608°F (320°C). The strength increases are due to the increasing complexity of the microstructure with irradiation. Irradiation induced defects such as faulted and glissile dislocation loops, voids, bubbles and fine precipitates increase in size and/or number density with neutron exposure. These act as hard barriers to dislocation motion, and increase the stress necessary for plastic deformation.

Ultimate tensile strength also increased in the program materials with increasing accumulation of irradiation damage, though to a lesser degree than yield strength. Well-annealed 304SS exhibits an ultimate tensile strength of about 80 to 85 ksi (550 to 590 MPa) at room temperature. The very low fluence specimens, however, were slightly stronger with ultimate tensile strengths of roughly 95 ksi (660 MPa). This increase can be attributed to strain hardening that occurred as the austenitic steel transformed to martensite during extensive plastic deformation. The effects of this phase transformation are manifested more obviously in the specimens' ductilities, and a more thorough discussion follows. Ultimate tensile strength increased with increasing neutron fluence, saturating with an increase of 80% at room temperature and 190% at 608°F (320°C).

At room temperature, although the yield strengths and ultimate tensile strengths became very similar at high fluence, the yield point and onset of necking did not coincide or approach one another. In other words, the specimens yielded at a low strain followed by a slight drop in load, then preceded to elongate and strain harden slightly as the martensite phase formed. This effect was not observed at elevated temperatures: at 4.5 dpa and above, the yield strength and ultimate tensile strength occurred at the same point on the stress strain curve.

The saturation fluence and strength levels are comparable to those of Types 304 and 316-cold worked and Type 347-solution annealed, austenitic stainless steels previously investigated in other MRP programs. The saturation level for both the yield and ultimate strengths at room temperature were found to be about 150 ksi (1030 MPa) above 5 dpa. At 608°F (320°C) the saturation strength levels were 130 ksi, (900 MPa) again above 5 dpa. A common saturation level for different types of austenitic stainless steels is reached because the fine, dense defect structure produced by irradiation overrides the solution or work hardening mechanisms present in the unirradiated steels.

EdF has reported [4] data from several heats of solution annealed 304 stainless steel. The yield strength for these materials, irradiated in the fast spectrum BOR60 reactor, was found to saturate at a lower strength than was found in this program. They also report [5]. Chooz A 304 stainless steel irradiated 608°F (320°C) equivalent yield strength of ~130 ksi, (~900 MPa) presumably in the saturated region. A comparison of the data indicates that the PWR irradiated material may saturate at a slightly higher level than the BOR fast reactor irradiated material. However, this observation is based on very limited data and may be due to heat-to-heat variations or testing variability rather that the irradiation environment.

3.4.2 Ductility

The program 304SS exhibited very high uniform and total elongations at room temperature for all but the very highest levels of neutron exposure. This can most likely be attributed to the austenitic to martensitic phase transformation mentioned earlier. In austenitic stainless steels (γ, fcc), as localized stresses reach a threshold value they can be partially relieved by inducing a homogeneous shear in what will become the martensite platelet surface and a dilation normal to the habit plane, resulting in transformation to the martensitic (α', bcc) crystal structure [6]. This is a military, or diffusionless, transformation and takes place in an extremely small time interval. The mode of transformation seems to be as follows: a small localized volume of austenitic material reaches the threshold stress and transforms to martensite; the reduced section continues to elongate thereby bringing another localized volume of austenite to the threshold stress, this new volume is transformed, and so on until a large fraction of the reduced section is consumed. The extent of phase transformation in each specimen is unknown. Proof of the transformation is the magnetization of the deformed fracture surfaces. When a magnet is scanned over the length of a fractured room temperature tensile specimen the threaded ends respond very little, or not at all. The deformed region, however, is drawn towards the magnet with a force varying from sample to sample. This indicates that the threaded ends remained austenitic, while the deformed region transformed at least partially to a ferromagnetic phase, such as martensite.

Such a phase transformation is well documented for austenitic stainless steels [7, 8, 9], and is known to significantly enhance ductility. However, accounts of the extent of ductility seen in the low fluence, room temperature tests do not seem to be readily available. High variability in material ductility may be due to several factors. The spontaneous precipitation of martensite in austenite is prevented under zero-strain conditions by a free energy barrier in the form of surface energy creation and lattice strain energy, both of which increase the energy of the system with the precipitation and growth of a second phase. Sample stressing during the tensile test provides the lattice strain energy. During the phase transformation, these energy increases are balanced against the decrease in volume energy as the austenite transforms to the more stable martensite. The magnitude of this energy decrease depends on the concentration of solutes in the steel. As such, the energy barrier for precipitation and growth of martensite in an austenitic steel is strongly dependent on chemical composition, especially the amount of carbon, nickel, and chromium [6, 10]. Consequently, heat to heat variations as well as the yield stress will play a large role in the extent to which a specimen will undergo such a transformation, and at what point in the tensile test the transformation will happen.

A generally accepted measure of the tendency of an austenitic alloy to transform into martensite is the M_s temperature. This is the temperature below which martensite is the energetically stable phase. Again, chemical composition influences the M_s temperature strongly. It is obvious then that the test temperature is vitally important in the phase transformation consideration. Above the M_s temperature the austenite phase is stable at much higher stresses than for a low temperature test. If the temperature is high enough that the maximum true stress is lower than the stress necessary for phase transformation, martensite presence in the deformed region will be very limited, existing perhaps only in regions of localized material constraint. The specimens tested at 608°F did not exhibit the large amount of ductility seen at room temperature, and very little ferromagnetism seems to be present. High temperature, low fluence specimens had uniform elongations approximately half as large as their low temperature counterparts; and for fluences of roughly 4 dpa and greater, uniform elongation was virtually nonexistent at elevated temperature.

Dislocation structure has an additional influence on the extent of martensite transformation, as evidenced by cold-rolling experiments [10]. It is therefore likely that the irradiation induced defect structure plays some sort of role as well in determining the tendency towards phase transformation, and further that the interdependency of the defect structure strengthening and the martensitic phase transformation *together* shape the tensile properties.

The 608°F uniform and total elongation data is compared to similar data from other MRP programs. The uniform elongation is within the scatter of the other data after irradiation. For the total elongation, the results show slightly more ductility and it is not expected that the saturation level at higher fluences would be any lower than the 7% value found for the other investigations.

3.4.3 Fractography

Two specimens at ~12 dpa fluence showed little non-uniform elongation and, because the fractured specimens showed little evidence of necking, fractography was performed to investigate what appeared to be brittle failures. Both specimens were found to have failed mainly intergranularly, with small amounts of dimpled rupture. The circumferential perimeter of the fracture surface consisted of ductile dimpled-rupture, indicating that the intergranular failure mechanism was active only after high stress.

The occurrence of intergranular failure in the absence of a corrosive environment is unexpected. Currently, two hypotheses are being considered. First, hydrogen pick-up due to corrosion, coolant hydrogen and radiolysis of the reactor coolant may cause embrittlement of the program material. Because H solubility is lower and diffusivity is higher in martensite with respect to austenite, as the phase transformation occurs any dissolved H may be rejected into the remaining austenitic parent phase material, dramatically increasing the H concentration there. Also, radiation induced segregation (RIS) results in compositional changes in grain boundary chemistry (specifically Ni segregation and Cr depletion) that create a layer of material several nanometers thick with greatly increased austenite stability. It is likely that these two mechanisms somehow work synergistically to produce intergranular fracture morphology.

At both room and elevated temperature, the uniform and total elongations decreased sharply between fluence levels of ~0.03 dpa and ~0.06 dpa. The ductility of specimens at both test temperatures continued to decrease until they reached a saturation value at a fluence level between ~0.5 dpa and ~5 dpa. The highest fluence room temperature test showed a second sharp drop in ductility at ~12 dpa, but no equivalent room-temperature specimen was machined to determine if the total elongation would decrease similarly below the M_s.

3.4.4 Specimen Size Effect

Two specimens of similar neutron exposure and irradiation temperature but differing reduced section diameter were machined for elevated temperature testing, as a means of confirming the reliability of the data generated by the program's miniature specimens. The larger specimen was machined to 0.250 inches diameter and a smaller specimen was machined to the same 0.110 inch diameter as all other tensile and SSRT specimens in the program. Both were from the same orientation in the former plate. There was very little dissimilarity in the test stress-strain curves:

both specimens began necking immediately upon yielding, and all derived tensile properties were very similar. The larger specimen achieved a slightly higher yield/ultimate tensile strength, and failed less rapidly at the onset of advanced necking.

3.5 References

1. Characterization Report.
2. ASTM E8-98, "Standard Test Method for Tension Testing of Metallic Materials," ASTM, 1998.
3. ASTM E21-92, "Standard Test Method for Elevated Temperature Tension Tests of Metallic Materials," ASTM, 1992.
4. Massoud J-P, Dubuisson PH, Irradiations in BOR-60 reactor, Results of the Post Irradiation Tests and Investigations, Draft report EDF HT-27/03/018/A, August, 2003.
5. Robinot, P., Corniere de Cloisonnement de Chooz A, rapport d'estape No. 2 : essais de traction, essais de tenacite, note EDF-GDL D.5716/RBT/RA 95.6341, Indice 0,06 Fevrier, 1996.
6. Porter D. A., Easterling K. E., "Phase Transformations in Metals and Alloys," Van Nostrand Reinhold (UK) Co, Ltd., Berkshire, England, 1981.
7. Reed R. P., "The Spontaneous Martensitic Transformations in 18% Cr, 8% Ni Steels," Acta Metallurgica, Vol. 10, Sep. 1962.
8. Guntner C. J., Reed R. P., "The Effect of Experimental Variables Including the Martensitic Transformation on the Low Temperature Mechanical Properties of Austenitic Stainless Steels," Transactions of the ASM, Volume 55, 1962.
9. Maksimkin O. P., Tivanova O. V., "True Characteristics of Strength and Ductility for Neutron-Irradiated Metals and Alloys," *Effects of Radiation on Materials: 20th International Symposium, ASTM STP 1405,* S. T. Rosinski, M. L. Grossbeck, T. R. Allen, and A. S. Kumar, Eds., American Society for Testing and Materials, West Conshohocken, PA, 2001.
10. Carlsen K. M., Thomas K. C., "Effect of Composition, Heat Treatment and Cold Rolling on Mechanical Properties of Cr-Ni Stainless Steels," Transactions of the ASM, Volume 55, 1962.

4
SLOW STRAIN RATE TENSILE (SSRT) TESTING

Slow strain rate tensile tests are used in stress corrosion testing to accelerate the failure of susceptible materials to reasonable test times. The results generated are used as a qualitative indicator of relative corrosion resistance between different materials, or within one material as a means of evaluating changes in corrosion resistance with some physical process, such as microstructural evolution through heat treatment, cold working, or neutron irradiation. Several metrics that are useful for making such comparisons include time to failure, elongation to failure, maximum load, reduction in area, and in particular fracture morphology.

4.1 Test Procedure

Tests were performed in 340°C simulated PWR water at a constant extension rate of ~$1x10^{-7}$ mm/mm of effective gage length per second. Specimens were of the smaller design (Figure 3-2). The simulated PWR environment was deionized water with the following additions:

H_3BO_3 ~1000 ppm as B

LiOH ~2 ppm as Li

The following contaminants and conditions are controlled:

Dissolved oxygen <5 ppb

Dissolved hydrogen ~30 cm^3/kg H_2O at STP

Chlorine <30 ppb

Flourine <30 ppb

pH ~6.9 at room temperature

Conductivity of the deionized water <0.3 µS/cm

Total dissolved solids <0.2 ppm

Dissolved silica <0.1 ppm

During the test, the following data were recorded as a function of time:

- Water temperature near the gage section. For all tests, the temperature is constant within 2°C of the specified test temperature.
- Autoclave pressure.
- Extension of the load rod.
- Load on the load rod.

Water samples were taken of the autoclave run and water batch. These samples were analyzed for specific chemicals and their concentration in the water. Water flow was 100 to 200 ml/hr during the test.

4.2 Test Equipment

The SSRT test equipment consists of a test chamber, two parallel load application systems, a shield assembly, and a water system. These components are shown in Figure 4-1. The tests stand was specifically designed to allow for mounting of the specimen in the load frame inside of a hot cell. However, once loading is completed, the equipment assembly and the testing are conducted outside of the cell.

The test chamber is a standard 3.8 liter stainless steel 3,000 psi autoclave. For radiation shielding purposes, the autoclave has a specially designed head, which is 20 cm thick. The available head has penetrations for required instrumentation, and one or two loading rods. The load rods are sealed to the head with multiple O-rings.

The loading assembly consists of grip assemblies through which the specimen is pinned to the load rods. Load is supplied by a variable DC motor, which drives a series of gear reducers, then a screw jack. The screw jack converts the rotational motion of the motor to a linear motion in the load rod. The gear reducers are selected to convert the motor speed to the desired extension rate on the specimen. The motor speed can be adjusted to fine-tune the extension rate.

To allow testing outside of the hot cell, the test autoclave sits in a 20 cm thick shield. The shield and the top plate help form a secondary vessel, which is required for safety in the unlikely event that a seal would rupture.

The once-through water supply system consists of a high pressure pump, a make-up tank, and instrumentation to monitor the water pressure and conductivity. After the water circulates through the autoclave and is cooled, the pressure is reduced with a backpressure regulator.

4.3 Results and Discussion: Fractography of SSRT Specimens

The result of the SSRT test considered in this report is the measure of the intergranular/ transgranular cleavage stress corrosion cracking (SCC) on the specimen fracture surface. Fractography of the failed specimens was performed using a shielded Amray Scanning Electron Microscope (SEM). The fracture morphologies of the program materials are summarized in Table 4-1. Results are reported in terms of percentages of non-ductile (intergranular or transgranular cleavage) failure. It must be noted that although the SSRT test and fracture morphology measurements provide a useful qualitative measure of IASCC susceptibility, the factors relating to environmentally assisted cracking are very complex and may vary significantly with subtle differences in heat-specific chemistry and surface condition. With regard to the latter, as corrosion processes are dependent on the stress intensity at the crack tip, the crack growth rate and stress on the remaining intact ligament (both of which will determine the final amount of non-ductile failure) depend on the distribution of surface crack density and depth. As such, a certain amount of variability is inherent in the test and it is instructive to identify trends in the data rather than differences between individual data points.

Water supply console containing water tanks, high pressure pump, autoclave temperature controllers and sampling ports.

Shielded autoclave with two slow strain rate test systems for one, four-liter autoclave.

Water output console containing back-pressure regulator, pressure and temperature indicators and sampling ports.

Figure 4-1
SSRT Test Equipment

Table 4-1
SSRT Testing Conditions and Results

Material Source	Fluence (dpa)	Test Temp.		% Intergranular	% Transgranular
		(°F)	(°C)		
Top-of-Core	<0.1	644	340	Low	Med
Barrel	~0.5	644	340	Low	Med
Mid-Core Former	~10	644	340	Med	Low
Mid-Core Baffle	~14	644	340	High	Low
Mid-Core Baffle	~15	644	340	Med	Low
Mid-Core Baffle	~17	644	340	High	Low

Low = 0-10% Med = 10-25% High = >25%

Typical fractographs of specimen fracture surfaces are shown in Figure 4-2. SCC initiates on the surface of the stressed region of the specimen. At low fluences there is usually a mixture of transgranular and intergranular crack morphology, as shown in Figure 4-2. This program clearly shows that the transgranular component decreases with fluence and disappears probably somewhere in the 2 to 8 dpa range. The intergranular component, typically considered IASCC, usually initiates above ~1 dpa and increases with fluence. Depending on the test conditions, the increase in fracture intergranularity may be interrupted by a ductile overload (dimpled rupture morphology) failure. This would be expected to occur if the stress on the remaining ligament is increasing as the crack grows since the fracture toughness at high fluence is suspected to be greatly decreased. If the grain boundaries are weakened by the IASCC mechanism, then all or most of the fracture surface may fail intergranularly.

At very low fluences (~0.1 dpa) the 304 stainless steel displayed unexpected corrosion properties. Though this fluence was well below the recognized threshold for IASCC, the test result showed approximately 25 percent of the fracture surface had failed by either transgranular cleavage or intergranular failure. At ~0.5 dpa the amount of transgranular cleavage and intergranular surface had decreased but still existed. It is suspected that this response may not be related to irradiation, but the reason for the behavior is unknown.

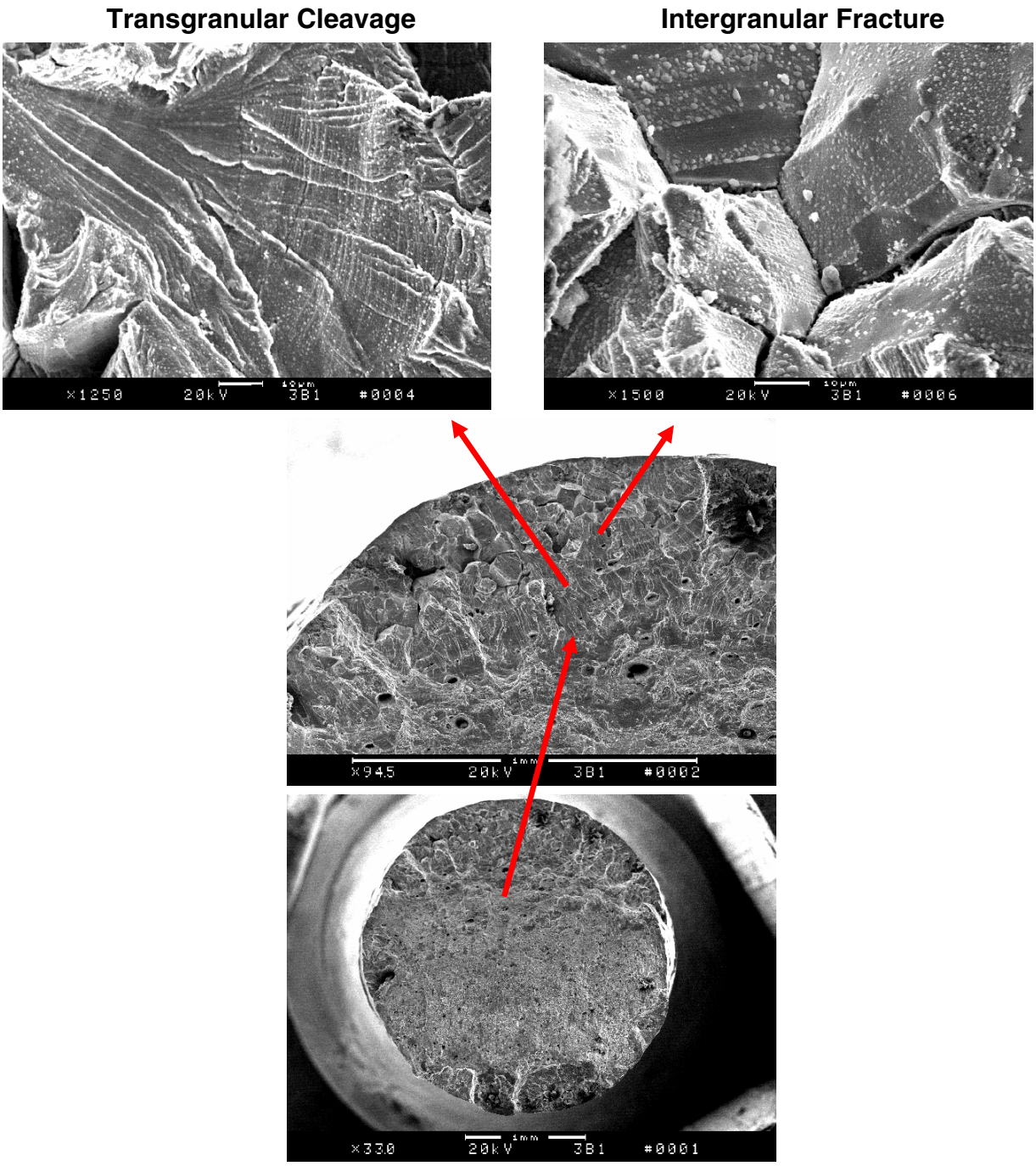

Figure 4-2
Typical Fractograph of Program Materials after SSRT Testing, Showing Regions of Intergranular Fracture, and Transgranular Cleavage

5
SUMMARY

Quantification of the evolution of mechanical and corrosion properties of structural austenitic stainless steel PWR internals is necessary to evaluate performance of vessel internals components of plants seeking life extension. This program represents the first time significant amounts of such material has been available for analysis. The results of this program will provide data free of the uncertainties implicit in fast-reactor exposure and irradiation in environments other than the PWR core. Data from the tensile testing and SSRT testing in this program is used to develop a database for Type 304 stainless steel plate irradiated in the internals region of a PWR. This data is compared with similar data for other austenitic stainless steels irradiated by other means to assess data sets applicability to PWR use. Results from this program may be used to gage the impact of irradiation effects on PWR vessel internals components performance, and to provide data for PWR owners to justify extended plant operation beyond its designed life. Additionally, many of the tests to be performed on the program material (fracture toughness, crack initiation, crack growth rate, etc.) rely on accurate measures of the tensile properties in order to select appropriate testing parameters.

Tensile testing revealed that the yield strength and ultimate tensile strength of annealed 304SS at room temperature both increase as a result of neutron irradiation. Unirradiated values for room temperature yield strength (σ_Y) and ultimate tensile strength (T.S.) (from the retrieved material certification sheets) are σ_Y = 35 ksi (240 MPa), T.S. ≈ 80 ksi (550 MPa), respectively. Irradiation causes an increase in these values to $\sigma_Y \approx$ 140 ksi (965 MPa) at approximately 5 dpa, at which point the strength increase is nearly saturated. Unirradiated values for yield strength and ultimate tensile strength at 608°F (320°C) (by testing nearly unirradiated program material) are $\sigma_Y \approx$ 25 ksi (170 MPa), T.S. ≈ 65 ksi (450 MPa). Irradiation causes an increase in these values to σ_Y, T.S. ≈ 115 ksi (790 MPa) at approximately 5 dpa, at which point the strength increase is nearly saturated. At room temperature, and for high levels of neutron irradiation, the yield strength and ultimate tensile strength become similar, but yielding and necking do not coincide as a result of the high ductility enabled by a martensitic phase transformation from the austenitic parent phase. Specimens having the highest levels of irradiation (11.8 dpa and 12.6 dpa) failed intergranularly. At elevated temperature (608ºF, 320°C) there appeared to be very little or no martensitic phase transformation, and the yield point coincided with the onset of necking. Material strength at elevated temperature was lower than at room temperature. At elevated temperature there is a marked decrease in ductility compared with room temperature, however all specimens failed in a ductile manner. There is little change in properties as measured by tensile specimens of different sizes, in strength or in ductility. Tensile properties measured with the miniature 0.110 inch gage diameter specimens may be regarded as typical of those that would be obtained with a larger specimen design.

SSRT testing in simulated PWR water showed that both intergranular and transgranular cracking occurred in the low fluence specimens. 25 percent of the fracture surface of the nearly unirradiated specimen (0.077 dpa) indicated a brittle failure mechanism (18% intergranular and 7% transgranular). Percentages of both intergranular and transgranular fracture surface decreased between 0.077 dpa and 0.461 dpa, however this may be within the range of data scatter inherent in the SSRT test. For neutron fluences above ~0.5 dpa, no transgranular cracking was observed, and intergranular cracking increased to values between approximately 20 and 30 percent. Cracking in low-fluence specimens began as either transgranular or intergranular. Intergranular cracks generally transitioned to transgranular before final ductile overload.

6
CONCLUSION

6.1 Tensile Testing

- The yield strength and ultimate tensile strength of annealed 304SS at room temperature both increase as a result of neutron irradiation up to ~5 dpa. Saturation of the strength increase occurs at a higher fluence.
- At room temperature, and for high levels of neutron irradiation, the yield strength and ultimate tensile strength become similar, but yielding and necking do not coincide as a result of the high ductility enabled by a martensitic phase transformation from the austenitic parent phase.
- The highest levels of irradiation produced a sharply decreasing amount of total elongation to failure and virtually zero non-uniform elongation, although the specimen irradiated to ~12 dpa exhibited significant uniform elongation. Fractography revealed that these specimens failed intergranularly.
- At room temperature and low fluence, the program materials exhibited very high levels of ductility as a result of the phase transformation. The level of ductility decreased with increasing exposure to neutron irradiation, due to normal dislocation/defect interactions.
- At elevated temperature (608ºF) there was very little if any martensitic phase transformation. The yield point coincided with the onset of necking (ultimate tensile strength). Both values were lower than at room temperature.
- At elevated temperature there is a marked decrease in ductility compared with room temperature, however all specimens failed in a ductile manner.
- There is little change in properties as measured by tensile specimens of different sizes, in strength or in ductility. Tensile properties measured with the miniature gage diameter specimens may be regarded as typical of those that would be obtained with a larger specimen design.

6.2 SSRT Testing

- All of the program plate 304 stainless steels were found to be susceptible to IASCC.
- The degree of susceptibility appeared to be similar to that found for other grades of austenitic stainless steels in other MRP sponsored programs.
- At very low fluence levels, <0.5 dpa, unexpected brittle cracking occurred in the program specimens.

- The percentage of transgranular cleavage on the SSRT specimen fracture surfaces decreased with increasing fluence. From the data, no cleavage would be expected above an irradiation level of several dpa.
- Cracking in low-fluence specimens began as either transgranular or intergranular. Intergranular cracks generally transitioned to transgranular before final ductile overload.

A
CUTTING DIAGRAMS FOR ALL PROGRAM SPECIMENS

Specimen locations were chosen in an effort to obtain a broad spectrum of neutron exposure values, or specific neutron exposure values in some instances. Specimen orientations were chosen in such a way as to maximize material usage, while minimizing fluence gradients within each specimen. Knowledge of each specimen's location and orientation was preserved throughout the entire machining and testing process. Figure A-1 shows each of the final cutting diagrams used in the program. Individual specimens are labeled.

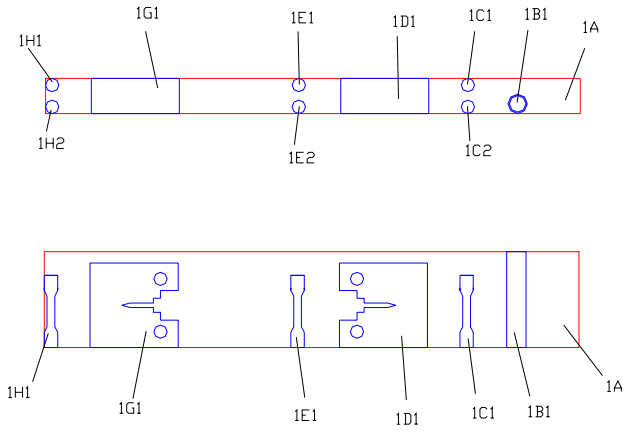

a) Baffle 1

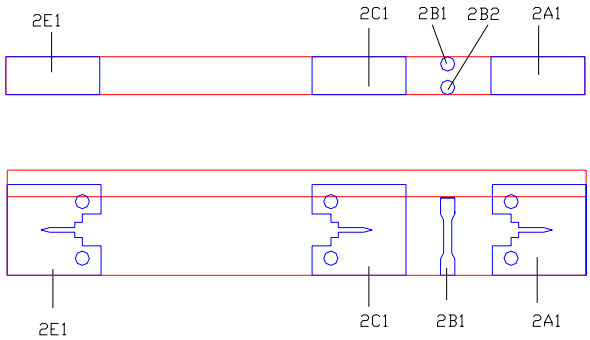

b) Baffle 2

Figure A-1
Cutting Diagrams for Program Materials (Not to Scale)

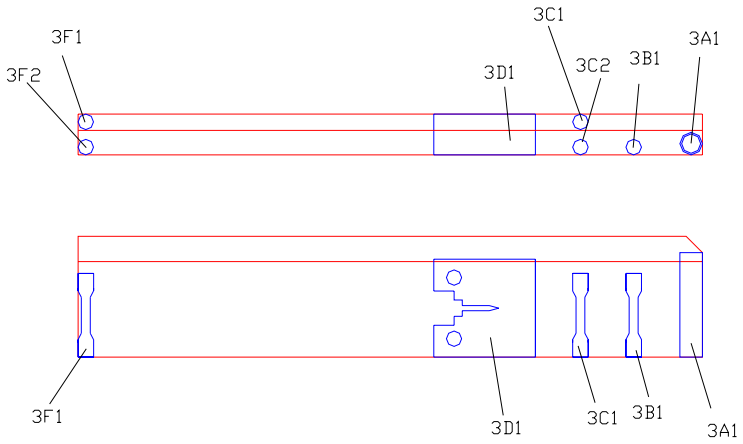

c) Baffle 3

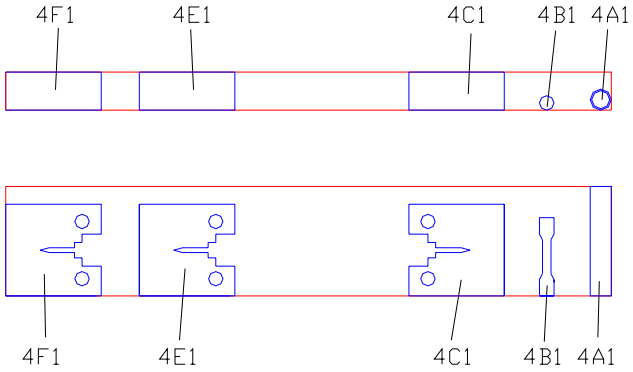

d) Baffle 4

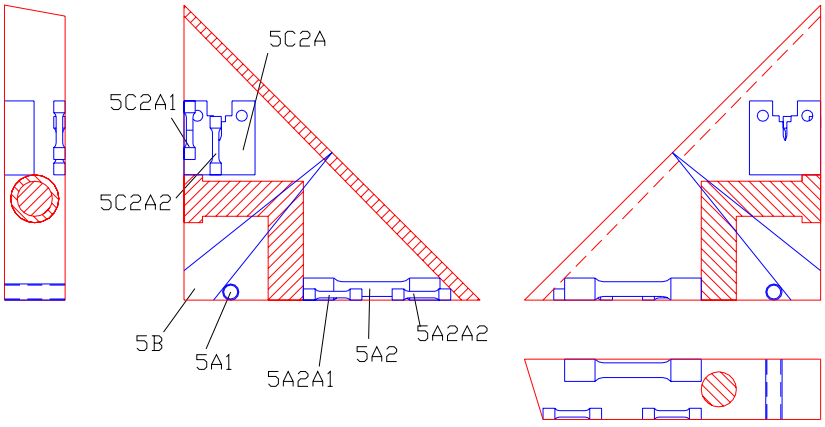

e) Former

Figure A-1
Cutting Diagrams for Program Materials (Not to Scale) (Continued)

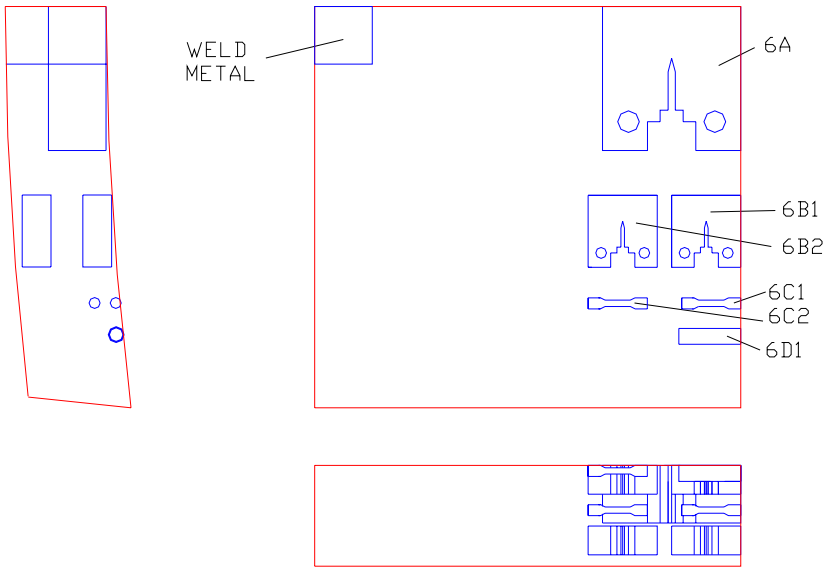

f) Barrel

Figure A-1
Cutting Diagrams for Program Materials (Not to Scale) (Continued)

Program:
Nuclear Power

About EPRI

EPRI creates science and technology solutions for the global energy and energy services industry. U.S. electric utilities established the Electric Power Research Institute in 1973 as a nonprofit research consortium for the benefit of utility members, their customers, and society. Now known simply as EPRI, the company provides a wide range of innovative products and services to more than 1000 energy-related organizations in 40 countries. EPRI's multidisciplinary team of scientists and engineers draws on a worldwide network of technical and business expertise to help solve today's toughest energy and environmental problems.

EPRI. Electrify the World

WARNING: This Document contains information classified under U.S. Export control regulations as restricted from export outside the United States. You are under an obligation to ensure that you have a legal right to obtain access to this information and to ensure that you obtain an export license prior to any re-export of this information. Special restrictions apply to access by anyone that is not a United States citizen or a Permanent United States resident. For further information regarding your obligations, please see the information contained below in the section entitled "Export Control Restrictions."

Export Control Restrictions

Access to and use of EPRI Intellectual Property is granted with the specific understanding and requirement that responsibility for ensuring full compliance with all applicable U.S. and foreign export laws and regulations is being undertaken by you and your company. This includes an obligation to ensure that any individual receiving access hereunder who is not a U.S. citizen or permanent U.S. resident is permitted access under applicable U.S. and foreign export laws and regulations. In the event you are uncertain whether you or your company may lawfully obtain access to this EPRI Intellectual Property, you acknowledge that it is your obligation to consult with your company's legal counsel to determine whether this access is lawful. Although EPRI may make available on a case by case basis an informal assessment of the applicable U.S. export classification for specific EPRI Intellectual Property, you and your company acknowledge that this assessment is solely for informational purposes and not for reliance purposes. You and your company acknowledge that it is still the obligation of you and your company to make your own assessment of the applicable U.S. export classification and ensure compliance accordingly. You and your company understand and acknowledge your obligations to make a prompt report to EPRI and the appropriate authorities regarding any access to or use of EPRI Intellectual Property hereunder that may be in violation of applicable U.S. or foreign export laws or regulations.

Printed on recycled paper in the United States of America

1011027

EPRI • 3412 Hillview Avenue, Palo Alto, California 94304 • PO Box 10412, Palo Alto, California 94303 • USA
800.313.3774 • 650.855.2121 • askepri@epri.com • www.epri.com